UNIVERSITY OF ARIZONA

Electrical Engineering Department, College of Engineering

Analog/Hybrid Computer Laboratory

ACL Memo No. 160

Hybrid-Computer Monte Carlo Techniques for Finding Eigenvalues of Partial Differential Equations

Richard D'Aquanni

September 1968

DRAFT

Abstract

This paper describes a Monte Carlo technique for estimating the lowest eigenvalues of certain elliptical partial differential equations with various boundary conditions. A stochastic process whose output conditional probability density distribution satisfies a partial differential equation similar to the partial differential equation under consideration is, along with the boundary conditions, implemented on ASTRAC II, a fast repetitive analog computer.

Eight different boundaries in one, two, and three-dimensional space were implemented, resulting in eight lowest-eigenvalue estimates, which are compared to the true lowest eigenvalues. Computer hardware errors, along with the error resulting from the mathematical approximation employed in deriving the estimate, are indicated. Corrective measures are included when necessary. Applications result from a presentation of analogies relating the partial differential equations under consideration to partial differential equations modeling physical processes.

I. INTRODUCTION

Numerical solutions for the lowest eigenvalues of certain partial differential equations are sometimes difficult to determine if one employs standard numerical techniques. A list of these standard techniques should include the finite difference method, Galerkin's method and the energy method of Rayleigh-Ritz.[13] Less standard, yet more sophisticated when applied to specific problems, are the methods of point matching or collocation,[17,20] segment matching[18], and conformal mapping.[16, 19]

A Monte Carlo method applied to lowest-eigenvalue estimation has been introduced and mathematically illustrated by Donsker and Kac.[1] Theoretically, Donsker and Kac suggested generation of a stochastic process (represented by generalized Langevin equations) resulting from the application of a white-Gaussian-noise forcing function to a first-order system, (see Appendix A). The conditional probability density function of the output variable (which completely describes the output process, since it is a first-order Markov process) satisfies Kolmogorov's backward partial differential equation. The determination of eigenvalues of various deterministic differential equations is based on these Kolmogorov backward partial differential equations.

In this paper, a stochastic process is generated, and applied in the estimation of the lowest eigenvalues of a number of geometric one, two, and three-dimensional boundaries representing the bodies under consideration. Realizing that randomness, the basis of Monte Carlo Methods, requires many repetitions for accurate and consistent estimates, we turn to the computer as the only feasible means to implement such a process. The computer to be employed is the second in a series of Arizona Statistical Repetitive Analog Computers, ASTRAC II.[3,4,5]

II. EXAMPLE PROBLEM

The implementation of one typical problem in detail will illustrate the Monte Carlo Technique employed. The sampling procedure and formula constituting the technique are common to all eigenvalue problems considered in this paper.

The problem considered is that of determining the lowest eigenvalue of a vibrating string. The linear partial differential equation governing small transverse vibrations of an elastic string under fixed constraints is:[14]

$$\frac{\partial^2 U(x,t)}{\partial x^2} = \frac{\partial^2 U(x,t)}{\partial t^2} \tag{1}$$

where U(x,t) is the transverse vibration amplitude at position x at time t, and where the normally encountered coefficient $c^2 = T/\rho$ has been normalized to unity through a linear transformation in the x coordinate.

The boundary conditions on the above equation will be taken as

$$\begin{aligned} U(-10,t) &= 0 \qquad (t \geq 0) \\ U(10,t) &= 0 \end{aligned} \tag{2}$$

and the initial condition is

$$U(x,0) = f(x) \qquad (-\ 10 \leq x \leq 10) \tag{3}$$

The computer set-up for the above problem is given in Figure 1. First observe the zero-mean (capacitor-coupled) one dimensional guassian distributed random walk resulting from the integration of a binomially distributed random square wave. N(T), the random square wave has a variance $2D_n$ empirically measured as 30×10^{-6} volts^2-sec.[2,13] Transitions in the amplitude of N(T) may occur only at times specified by the noise clock frequency used to drive the random noise generator. It is important to note that the random walk's smallest step size $y(\Delta T)$ is a function of the noise clock frequency, the amplitude of the random square wave and the integrator gain G or $1/_{RC}$. Next, observe how random walk excursions beyond either the + 10 volt or -10 volt fixed string boundaries are detected by use of two fast-analog-comparators. The logic gates and flip-flop following the comparators are necessary for resetting integrator and hence walk initial conditions. Finally, observe the binary counters and associated logic used in tallying both the number of walks completed and the number of walks resulting in boundary absorbtion corresponding to total walk time, "T_i".

Typical waveforms appearing in the simulation are given in Figure 2. Figure 2A illustrates the basic timing pulse $\overline{R}$ which sets the repetition rate and the length of the random walks. T_i may be varied by similarly varying the duty cycle of $\overline{R}$.

In Figure 2B, the random walk is shown along with the absorption boundary levels, $\pm$10 volts. In the first frame of the diagram, an absorption at the +10 volt boundary has occurred. In the second frame, no absorption has occurred during the time interval allotted for the walk, and the signal is reset at the end of this interval marked by $\overline{R}$. In the third frame, the signal has reached the -10 volt level; the walk stops at this point and the integrator is reset to its starting position once again. Figures 2C and D show the comparator outputs which correspond to a +10 volt and -10 volt absorption, respectively. Figure 2E shows the integrator mode timing signal corresponding to the signals shown in Figures 2B, C and D.

Figure 2F indicates the pulses inputted to the binary counter corresponding again to Figures 2B, C and D. Figure 2G indicates waveform R' which controls the number of repetitions and time between repetitions.

In general, the dimensionality of the boundary or describing partial differential equation would require just that many independent noise sources with boundaries for each variable. Implementation of two and three dimensional boundaries are illustrated in Figures 3A and 3B respectively.

The one dimensional random walk (Wiener Levy process) implemented in the above example satisfies the following stochastic differential equation of motion:

$$\frac{dy(T)}{dT} = GN(T) \tag{4}$$

known as the Langevin equation.[7,9,12]

This equation corresponds to a Markov process with its probability density satisfying Kolomogorov's partial differential equation[7,9,12] given as:

$$G^2 D_n \frac{\partial^2 U(x,t)}{\partial x^2} =- \frac{\partial U(x,t)}{\partial t} \tag{5}$$

Introducing the normalized time variable

$$T = t/G^2 D_n$$

Equation 4 may be written as:

$$\frac{\partial^2 U(x,T)}{\partial x^2} = - \frac{\partial U(x,T)}{\partial T} \tag{6}$$

As described in the Appendix, satisfaction of Equation 6 with the probability desnity of Equation 4 results in the following estimate for the lowest eigenvalue, λ,:

$$\hat{\lambda}_1 = \sqrt{\frac{\ln \frac{N_{t_1}}{N_{t_2}}}{t_2 - t_1}}$$

where N_{t_i} is the number of walks which remain within the boundaries during the time interval $(0, t_i)$ Note that N_{t_i} is calculated from the number of walks absorbed out of the total number of walks completed. This information is outputed from the computer simulation.

III. EXPERIMENTS WITH VARIOUS BOUNDARIES

A. Experimental Design

Proper utilization of our eigenvalue estimates, given by Equation B depends upon the correct choice of t_1 and Δt and hence on the choice of T_1, ΔT, and on our random step size "y". The sensitivity of the estimate variations in random walk source point and on dimensional boundary changes should also be determined if the estimate is to apply to the determination of lowest eigenvalues for boundaries of any shape and size.

Since time increments, step size, and possibly random walk starting point are all correlated, two initial choices were made:

1) Start all random walks from a point more or less centered with respect to the boundary.

2) Choose a step size of 0.5 volts, based on a 20 volt (± 10) boundary in all directions.

The criterion employed in initially selecting ΔT was to choose a ΔT covering the largest percent change in N_t while remaining within existing computer time limits. Figure 4, which is a plot of N_t vs. $T = t/DG^2$ for a one-dimensional boundary, was utilized in making an initial decision. Also included in Figure 4 is a plot for the curve $e^{-\lambda^2 T}$, where λ is the true eigenvalue. As expected, the curves agree quite closely. Trial of several combinations of T_1 and ΔT yielded $T_1 = 125\ \mu$ sec. and $T_2 = 525\ \mu$ sec. as values which produced the best estimate for our one dimensional boundary. These values were also chosen to represent all T values in two and three dimensions in the ± 10 volts bounded, 0.5 volt step size, cases.

Statistically, the estimated eigenvalue "λ" converges to the true eigenvalue as the sample size "N" increases.

ASTRACT II enables the user to take up to 1,000 walks/second with fast multipliers, comparators, and digital logic to accomodate this high repetition rate. I chose to take a fixed 10,000 samples, thus taking full advantage of ASTRACT II's speed while assuring statistical convergence.

B. Parameters, Estimates and Errors

The boundaries considered in this paper and their corresponding true eigenvalues are tabulated in Table 1. The parameters, final estimates, and associated errors for each boundary are shown in the fixed tabular block forms given below. The one dimensional boundary is given special treatment in that graphs indicating the eigenvalue estimate's probability density distribution and the effect on the estimated value due to variations in the random walk source point are presented. Also, the terminology used in all tabular blocks will be presented here.

1. Numerical Parameters, Results, and Errors

A. One Dimensional Boundary or Vibrating String

T_1 = 125 u sec

T_2 = 525 u sec

ΔT = 400 u sec

y = 0.5 volts/u sec

N = 10,000 walks

f_R = 1000 walks/sec

$f_{\text{noise clock}}$ = 1M Hz

t/T = 0.125×10^6

$\hat{\lambda}_{29}$ = 0.166485 for $y_o = 0$

s^2 = 4.19×10^{-5}

s = 6.47×10^{-3}

ϵ = 5.98%

where: (1) $\hat{\lambda}_m$ is the estimated Eigenvalue based on m samples of 10,000 walks each

(2) S^2 is the sample variance

$$S^2 = \overline{\hat{\lambda}_m^2} - (\overline{\hat{\lambda}_m})^2$$

(3) S is the sample standard deviation

$$S = \sqrt{S^2}$$

(4) ϵ is the error of the estimated Eigenvalue from its true value.

$$\epsilon = \frac{|\lambda_t - \hat{\lambda}_m|}{\lambda_t}$$

In addition to the above results, Figures 5 and 6 indicate the normally distributed density of the estimated eigenvalue, and the variation in the estimate with changes in the walk source point, respectively. Although only 29 eigenvalues were estimated, Figure 5 does indeed indicate an approximately normal distribution with mean range including the true mean eigenvalue. Figure 6 indicates that all sample eigenvalues are geometrically insensitive, i.e., less than 5% statistical error from true value, to initial random walk point variations within $\pm$16% from midpoint to boundary. Beyond $\pm$60%, the estimates became progressively inaccurate due to the failure of the circuitry to record a hit and reset the integrator at the rapid rate at which the boundary hits occurred.

2. <u>Two Dimensional Circular Boundary</u>

T_1 = 125 u sec	N = 10,000 walks
T_2 = 525 u sec	f_R = 1,000 walks/sec
ΔT = 400 u sec	$f_{noise\ clock}$ = 1 M Hz
y = 0.5 Volt/u sec	t/T = 0.125×10^6

$$\hat{\lambda}_5 = 0.226649 \text{ for } (x_o, y_o) = (0,0)$$

$$S^2 = 0.90 \times 10^{-6}$$

$$S = 9.48 \times 10^{-4}$$

$$\epsilon = 5.75\%$$

For $\hat{\lambda}_5$ originating at $x_o = 0$; $y_o = 0.5, 1, 2, 3, 4, 5$ and 6 volts No error from estimated value at (0,0) greater than 1.5% was recorded. See Figure 7A for photograph of walks within this boundary.

3. Two Dimensional Square Boundary

$T_1 = 125$ u sec

$T_2 = 525$ u sec

$\Delta T = 400$ u sec

$y = 0.5$ volts/u sec

$N = 10{,}000$ walks

$f_R = 1{,}000$ walks/sec

$f_{\text{noise clock}} = 1$ M Hz

$t/T = 0.125 \times 10^6$

$$\hat{\lambda}_5 = 0.218445 \text{ at } (x_o, y_o) = (0,0)$$

$$\epsilon = 1.66\%$$

For $\hat{\lambda}_5$ originating at $\begin{cases} x_o = 0;\ y_o = \pm.5,\ \pm1,\ \pm3 \text{ and } \pm5 \text{ volts} \\ \text{and} \\ x_o = y_o = \pm0.5,\ \pm1,\ \pm2,\ \pm3 \text{ volts} \end{cases}$

No error from estimated value at (0,0) greater than 3.45% was recorded.

4. Two Dimensional Rectangular Boundary

$T_1 = 125$ u sec

$T_2 = 525$ u sec

$\Delta T = 400$ u sec

$y = 0.5$ volts/u sec

$N = 10{,}000$ walks

$f_R = 1{,}000$ walks/sec

$f_{\text{noise clock}} = 1$ M Hz

$t/T = 0.125 \times 10^6$

$\hat{\lambda}_5 = 0.231229$ at $(x_o, y_o) = (0,0)$

$\epsilon = 7.99\%$

For $\hat{\lambda}_5$ originating at (2, 1.5) an error of 2.9% from estimate at (0,0) was recorded. See Figure 7B for photograph of walks within this boundary.

5. Two Dimensional Circular Boundary with One Vane

T_1	=	1250 u sec	N	=	10,000 walks
T_2	=	5250 u sec	f_R	=	100 walks/sec
ΔT	=	400 u sec	f_{noise} clock	=	100 K Hz
y	=	0.5 volts/ 10 u sec	t/T	=	0.125×10^7

$\hat{\lambda}_5 = 0.223796$ at $(x_o, y_o) = (1,0)$

$\epsilon = 3.47\%$

6. Three Dimensional Spherical Boundary

T_1	=	125 u sec	N	=	10,000 walks
T_2	=	525 u sec	f_R	=	1,000 walks/sec
ΔT	=	400 u sec	f_{noise} clock	=	0.5 M Hz
y*	=	0.5 volts/ 2 u sec	t/T	=	0.0625×10^6

$\hat{\lambda} = 0.321350$ for $(x_o, y_o, z_o) = (0,0,0)$

$\epsilon = 2.39\%$

For $\hat{\lambda}$ originating at (1,1,1) an error of 2.22% from estimate at (0,0,0) was recorded.

7. <u>Three Dimensional Cubical Boundary</u>

T_1 = 125 u sec

T_2 = 525 u sec

ΔT = 400 u sec

y^* = 0.5 volts/ 2 u sec

N = 10,000 walks

f_R = 1,000 walks/sec

$f_{noise\ clock}$ = 0.5 M Hz

t/T = 0.0625×10^6

$\hat{\lambda}_5$ = 0.250788 for $(x_o, y_o, z_o) = (0,0,0)$

ϵ = 7.82%

For For $\hat{\lambda}_5$ originating at (1,1,1) an error of 0.235% from estimate at (0,0,0) was recorded.

8. <u>Three Dimensional Cylindrical Boundary</u>

T_1 = 200 u sec

T_2 = 800 u sec

ΔT = 600 u sec

$y.$ = 0.5 volts/ 2 u sec

N = 10,000 walks

f_R = 1,000 walks/sec

$f_{noise\ clock}$ = 0.5 M Hz

t/T = 0.0625×10^6

$\hat{\lambda}$ = 0.280305 for $(x_o, y_o, z_o) = (0,0,0)$

ϵ = 2.41%

For $\hat{\lambda}_5$ with walk originating at (1,1,1) an error of 0.259% from estimate at (0,0,0) was recorded.

---

*Here an integrator input resistance equal to 2K rather than the normally used 1K input resistor was employed.

IV. Error Sources

A. Estimate Approximation Error

Our lowest eigenvalue estimate repeated here for convenience.

$$\hat{\lambda}_1 = \sqrt{\frac{\ln\frac{N_{t_1}}{N_{t_2}}}{t_2 - t_1}}$$

is based on the assumption that both t_1 and t_2 are large, thus enabling the higher order eigenvalue expontentials to approach zero. With our values of t_1 = 15.625 sec and t_2 = 65.625 sec this error is negligible.

B. Equipment Considerations

1.) Our noise source has a bandwidth of 500 KHz which, compared to the 30 MHz bandwidth of ASTRAC II amplifiers, is the band limiting device in our study. The white-noise assumption is, however, valid for sufficiently long steps (i.e., by increasing G) thus insuring independence between steps and hence randomness.

2.) At the very start of the random walks, the mean or d.c. component of the random noise source is not properly filtered out by the slowly charging 10 uf. capacitor. Although this initial charging time could lead to erroneous biased random walks, it was easily overcome by merely running the computer until the capacitor was fully charged, prior to any recordings.

3.) Amplifier drift errors were kept below 1% of 10v. (100 mv) by ensuring that the offset voltage K satisfied:[2]

$$K \leq 10^{-3} 2D_N G \tag{5}$$

Notice for f_R= 1000 runs/sec and $f_{noise\ clock}$ = 1 MHz or for f_R = 100 runs/sec and $f_{noise\ clock}$ = 100 KHz with R_{input} = 1K in both cases, the value for $2D_N G$ is 3.0×10^{-3}. For the amplifiers used in ASTRAC II, $K \leq 20 \times 10^{-5}$, which is well within the conditions of Equation 9.

4.) ~~The~~ The comparators and logic must respond quickly enough in recording a boundary hit and resetting all integrators before another step occurs. ASTRAC II's fast comparators and logic do indeed accomplish this feat within less than 1 u sec, within the smallest possible time for a step with the fastest noise-clock frequency of 1 MHz.

5.) Because comparator static hysteresis (10 millivolts), requires a boundary absorption rather than just a hit for detection, a boundary hit for a one-dimensional boundary has a small probability

$$\left[1 - \left(\sum_{i=1}^{N} \binom{i}{\frac{i+1}{2}} \left(\frac{1}{2}\right)^{i}\right)\right]$$ where 1) is always odd and $\leq N$ and 2) $N = t/T_{noise\ clock}$

of not crossing the boundary in time "t" remaining after a boundary hit, and thus boundaries are defined only within ± 10 mv. This applies to multi-dimensional boundaries as well.

6.) As expected, (Fig. 8) estimate errors as a result of small noise-step sizes exist due to the increasing dominance of computer drift, while truncation errors become significant as larger step sizes are employed. Also, the small number of binary distributed random step events tallied over our fixed time interval results in a poor binomial approximation to a normal distribution. This last error may be reduced by choosing $T_1 = (^{0.5}/x)$ 125 u seconds and $T_2 = (^{0.5}/x)$ 525 μ seconds.

V. APPLICATIONS

As mentioned previously, the partial differential equations considered may describe a variety of physical processes including the vibration of a spring or two dimensional membrane, or the motion of electromagnetic waves in a waveguide or of neutrons in a nuclear plant.

The first application concerns the determination of cutoff frequencies of waveguides. Although applicable to waveguides of any cross-sectional contour, this Monte Carlo technique compares with, and in some ways surpasses, other techniques when applied to cross-sectional contours for which closed form solutions obtained through classical methods are non-existent. The importance of this application may be observed by noting the operational advantages in employing an arbitrarily contoured cross-sectional waveguide.[16]

The propagation of an electromagnetic wave in a waveguide in an axial direction as shown in Figure 9 is mathematically represented by Helmholtz's partial differential or wave equation:

$$\nabla^2 \Psi(x,y) + k_i^2 \,\Psi(x,y) = 0$$

where: $\Psi(x,y)$ is the potential function

∇^2 is the two-dimensional Laplacian Operator

K_i's are real discrete frequency parameters representing cutoff frequencies analytically given as:

$$K^2 = K_o^3 - K_z^2$$

$$K_o^2 = \omega^2/\mu_o \epsilon_o$$

$$K_z^2 = 2\pi/\lambda_g$$

λ_g defined as the waveguide wavelength

In the T.M. wave mode

$$\Psi[L(x,y)] = 0$$

where: $L(x,y) = 0$ is the equation of the boundary of cross section.

The solution of the wave equation with the above boundary condition for the lowest cutoff frequency K_1, may be accomplished through utilization of the Monte Carlo technique and in fact yields the eigenvalue describing the first mode of vibration of the two-dimensional membrane described by the wave equation.

A second application concerns the criticality problem associated with nuclear reactors. The criticality problem asks whether a pulse of neutrons when injected into a nuclear reactor assembly will cause a multiplying chain reaction or will merely be absorbed. More specifically, it is concerned with the size of the assembly at which reaction is just able to sustain itself.

The criticality constant defining a subcritical, cirtical or supercritical combination reactor assembly and absorbent material can be determined by making a simple comparison between a directly measureable quantity known as the material buckling coefficient and the geometric buckling coefficient B_g,(22.

B_{g_1} is mathematically given by(21):

$$B^2_{g_i} = \frac{-\nabla^2 R(r)}{R(r)}$$

or as:

$$\nabla^2 R(r) + B^2_{g_i} R(r) = 0$$

where: $R(r)$ describes the neutron flux density at coordinate position $\bar{r}$.

∇^2, is the three-dimentional Laplacian operator.

The criticality problem is indeed an eigenvalue problem[8] as we recognize that the solution of the above standing-wave equation for G_{g_1} yields the eigenvalue describing the first mode of bibration of the three-dimensional body.

Just as the lowest eigenvalue solutions to the partial differential equations describing motion of membranes are subject to the boundary conditions that the edges of the membranes are in a fixed position, so too are the buckling coefficient solutions to the partial differential equations describing the neutron density distribution in an operating reactor subject to the boundary condition that the flux must approach zero along the boundary of the reactor.[22]

VI. CONCLUSION

The feasibility of a Monte Carlo method applied toward the estimation of lowest eigenvalues of partial differential equations has been demonstrated. The accuracy of all eight estimates (<8 percent) appear to satisfy engineering needs where close approximations are usually sufficient.

The availability of fast-repetitive analog computers such as ASTRAC II makes this method potentially attractive. With these computers, we are able to solve partial differential equations for their lowest eigenvalues with, as compared to current methods, a minimum amount of computation time. This is especially attractive for multidimensional problems.

ACKNOWLEDGMENT

The author is indebted to Professor Granino A. Korn for his knowledgable suggestions and direction, and to Dr. Howard Handler for both his uncovering and preliminary implementation of this method.

REFERENCES

1. Donsker, M.D., and M. Kac, The Monte Carlo Method and Its Application, Computation Seminar, Cornell University, pp. 74-80.

2. Handler, H., High Speed Monte Carlo Technique for Hybrid-Computer Solution of Partial Differential Equations, Ph.D. dissertation, Dept. of Electrical Engineering, University of Arizona, January 1967.

3. Korn G. A., and T. M. Korn, Electronic Analog and Hybrid Computers, McGraw-Hill, New York, 1964.

4. Eckes, H. R., and G. A. Korn, Digital Program Control for Iterative Differential Analyzers, Simulation Vol. No. February, 1964, pp. 33-41.

5. Korn, G. A., Random Process Simulation and Measurements, McGraw-Hill, New York, 1966.

6. Papoulis, A., Probability, Random Variables and Stochastic Processes, McGraw-Hill, New York, 1965.

7. Feller, W., An Introduction to Probability Theory and Its Applications, Second Edition, Volume I, Wiley, 1957.

8. Hammersley, J. M., and D. C. Handscomb, Monte Carlo Methods, Methuen's Monographs on Applied Probability and Statistics, Wiley, New York, 1964, pp. 98, 99, 104-106.

9. Wax, N., Selected Papers on Noise and Stochastic Processes, Dover, New York, 1954. Papers by Ming Chen Wang and G. E. Ohlenbeck.

10. Fortet, R., On the Estimation of an Eigenvalue by an Additive Functional of a Stochastic Process, with Special Reference to the Donsker-Kac Method, Journal of Research of the National Bureau of Standards, Vol, 48, No. 1, January, 1952, pp. 68-75.

11. Wasow, W., Random Walks and the Eigenvalues of Elliptic Difference Equations, Journal of the National Bureau of Standards, Vol. 46, No. 1, January 1951, pp. 65-73.

12. Korn, G.A., and T.M. Korn, Mathematical Handbook for Scientists and Engineers, McGraw Hill, New York, 1961

13. Little, W. D., and A. C. Soudack, Boundary Generation and Detection in Random Walk Problems, Simulation, Vol. 7, No. 2 August, 1966, pp. 63-65.

REFERENCES (Con't)

14. Kreyszig, E., Advanced Engineering Math, Wiley, 1962.

15. Rubin, E. I., Hybrid Techniques for Generation of Arbitrary Functions, Martin Mariette Report, Martin Company, Baltimore, Maryland.

16. Chi, M. and P. A. Laura, Approximate method of determining the cutoff frequency of waveguides of arbitrary cross sections, IEEE Transactions, Microwave Theory and Techniques (Correspondence), Vol. M.T.T.-12, March, 1964, pp. 248-249.

17. Laura, P.A., Determination of Cutoff Frequencies of Wave-guides with Arbitrary Cross Sections by Point Matching Proceeding's of the I.E.E.E. (correspondence) Vol. 53, No. 10, October 1965

18. Laura, P. A., A simple method for the determination of cutoff frequencies of waveguides with arbitrary cross sections, Proceedings of the IEEE (letters) Vol. 54, No. 10, October, 1966, 1495-1497.

19. Casarella, M. J. and P. A. Laura, Determination of Cutoff Frequencies of Grooved Waveguides, Proceedings of the IEEE (letters), Vol. 55, No. 6, June, 1967, pp. 1096-1097.

20. Laura, P.A., Application of the Point Matching Method in Waveguide Problems, I.E.E.E. Transactions on Micro-Wave Theory correspondence, May, 1966, Vol. M.T.T.-14 No. 5

21. Glqsstone, and Edlund, The Elements of Nuclear Reactor Theory, Van Nostrund, New York, 1952, pp. 194-215.

22. Dessauer, G. What is Buckling?, Nuclear News - ANS - September 1964, pp. 43-47.

APPENDIX A

This appendix describes the theory which yields the eigenvalue of boundary value problems.

Consider the following problem,

$$L_{\bar{r}}\, U(\bar{r}) + k^2 U(\bar{r}) = 0 \tag{A.1}$$

where $U(\bar{r})$ is defined within a bounded region R. On the boundary C, of R, the function $U_c(\bar{r}_b)$ is defined to be zero. The non-trivial solutions of (A.1) which satisfy this boundary condition are called the eigenfunctions of the problem, and the corresponding values of k are, the eigenvalues. The problem is to formulate a Monte Carlo procedure to calculate the lowest eigenvalue of (A.1). It will be assumed that the differential operator is such that:

a) the eigenvalues k, are real (L is Hermitian)

b) the operator L will yield a discrete set rather than a continuous spectrum of eigenvalues.

The generalized time invariant operator $L(\bar{r})$ is given below for an n dimensional space.

$$L(r)U(r) = - \sum_i \frac{\partial}{\partial r_i}\left[C_i(r)U(r)\right] + \frac{1}{2}\sum_{j,\ell} \frac{\partial^2}{r_j r_\ell}\left[D_{j\ell}(r)U(r)\right] \tag{A.2}$$

Conceptually, it is perhaps easiest to discuss this problem in two dimensions; however, the procedure holds for n dimension providing that the region R and its boundary are properly defined.

Consider a two-dimensional random walk originating at an interior point (x_o, y_o) of R. Let $Q(x_o, y_o, t)$ denote the probability that the particle will not be absorbed (stay within the boundary) in a time t given that the walk starts at a time t = 0.

Now,

$$Q(x_o, y_o, t) = \int_R\int p(x, y, t\ x_o, y_o) dxdy \tag{A.3}$$

where $p(x, y, t/x_o y_o)$ represents the probability density that at time t the particle performing the random walk is at point (x, y) given that it originated at (x_o, y_o). Integration over the entire region R produces the probability that the particle remains within the absorbing boundary C.

Since we are dealing with a Markov process (by assumption), the conditional density function $p(x, y, t/x_o, y_o)$ satisfies Kolmogorov's foward partial differential equation.( )

$$\frac{\partial}{\partial t} p(x, y, t/x_o, y_o) = L_{x,y}\, p(x, y, t/x_o, y_o) \tag{A.4}$$

with the following conditions.

$p(x, y, t/x_o, y_o) = 0$ on C for $t \neq 0$

i.e., the boundary is an absorbing one

$$p(x,y,t/x_o,y_o) \longrightarrow \delta(x-x_o)\delta(y-y_o) \text{ as } t \to 0$$

where δ denotes the Dirac delta function.

The general form of equation (A.4) is the following

$$\frac{\partial p(\bar{r},t/\bar{r}_o,t_o)}{\partial t} = -\sum_i \frac{\partial}{\partial r_i}\left[C_i(\bar{r},t)p(\bar{r},t/\bar{r}_o,t_o)\right]$$

$$+\frac{1}{2}\sum \frac{\partial^2}{\partial r_m \partial r_\ell}\left[D_{m,\ell}(\bar{r})p(\bar{r},t/\bar{r}_o,t_o)\right] \qquad (A.5)$$

where
the terms $C_i(\bar{r})$ and $D_{m,\ell}(\bar{r})$ are obtained from the generalized Langevin equations ( ) given below.

Considering a three dimensional case, $r_1 = x$, $r_2 = y$, $r_3 = z$, we have

$$\frac{dx}{dt} + A_1(x,y,z,t) = B_1(x,y,z,t)N_1(t) \qquad (A.6)$$

$$\frac{dy}{dt} + A_2(x,y,z,t) = B_2(x,y,z,t)N_2(t) \qquad (A.7)$$

$$\frac{dz}{dt} + A_3(x,y,z,t) = B_3(x,y,z,t)N_3(t) \qquad (A.8)$$

It is assumed that both A_i and B_i vary slowly with time when compared to the rapid variations of $N_i(t)$. The noise terms $N_i(t)$ are uncorrelated stationary white gaussian noise sources with zero mean and power spectral density $2Dn_i$.

The relationship between the coefficients of the Langevin equations and the terms in the operator L(r) is given by

$$C_1(\bar{r},t) = -A_1(\bar{r},t) \tag{A.9}$$

$$C_2(\bar{r},t) = -A_2(\bar{r},t) \tag{A.10}$$

$$C_3(\bar{r},t) = -A_3(\bar{r},t) \tag{A.11}$$

$$D_{11}(\bar{r},t) = 2Dn_1 B_1^2(\bar{r},t) \tag{A.12}$$

$$D_{22}(\bar{r},t) = 2Dn_2 B_2^2(\bar{r},t) \tag{A.13}$$

$$D_{33}(\bar{r},t) = 2Dn_3 B_3^2(\bar{r},t) \tag{A.14}$$

$$D_{12} = D_{13} = D_{23} = 0 \tag{A.15}$$

If the operator L_{xy} in equation (A.4) is of such a nature that the method of separation of variables can be applied to the partial differential equation, then we assume that

$$p = T(t)U(x,y) \tag{A.16}$$

Substitution in Eq. A.4 yields

$$T'(t)U(x,y) = T(t)L_{x,y}U(x,y) \tag{A.17}$$

Division of both sides of the above equation by

$T(t)U(x,y)$ gives

$$\frac{T'(t)}{T(t)} = \frac{L_{xy}\,U(x,y)}{U(x,y)} \tag{A.18}$$

Since the space coordinates do not appear in the left hand side and time does not appear in the right hand side, both sides of the equation are set equal to a constant, $-k^2$

$$\frac{T'(t)}{T(t)} = -k^2 \tag{A.19}$$

Equation (A.19) yields solutions of the form

$$T(t) = \exp(-k^2t) \tag{A.20}$$

The other equation which results from this technique is

$$L_{x,y}U(x,y) + k^2U(x,y) = 0 \tag{A.21}$$

Where $U(x,y)$ is zero for (x,y) on the boundary, which results from the condition that $p(x,y,t/x_o,y_o) = 0$ on the boundary

Equation (A.21), along with the boundary conditions yields a set of orthonormal functions, $\Psi_j(x,y)$ corresponding to values of $k = k_j$.

The solution to (A.4) can be written in series form in terms of the eigenvalues and eigenfunctions as,

$$p(x,y,t/x_o,y_o) = \sum_{j=1}^{\infty} A_j e^{-k_j^2 t} \Psi_j(x,y) \qquad \text{(A.22)}$$

Where the k_j's are assumed to be a decreasing discrete set of real numbers.

Using the initial conditions on the conditional density function $p(x,y,t/x_o,y_o) \longrightarrow \delta(x-x_o)\delta(y-y_o)$ as $t \rightarrow 0$ equation (A.22) may be written as

$$\delta(x-x_o)\delta(y-y_o) = \sum_{j=1}^{\infty} A_j \Psi_j(x,y) \qquad \text{(A.23)}$$

Multiplying both sides of the above equation by $\Psi_m(x,y)$ and integrating over R

$$\int_R\int \Psi_m(x,y)\delta(x-x_o)\delta(y-y_o)\,dxdy \qquad \text{(A.24)}$$

$$= \int_R\int \sum_{j=1}^{\infty} A_j \Psi_j(x,y)\Psi_m(x,y)\,dxdy \qquad \text{(A.24)}$$

If the series representation of the conditional density function (A.22) is uniformly convergent then the order of integration and summation can be interchanged, resulting in the following equation:

$$\Psi_k(x_o,y_o) = \sum_{j=1}^{\infty} A_j \int_R\int \Psi_j(x,y)\Psi_k(x,y)\,dxdy \tag{A.25}$$

Since the Ψ_k's are an orthonormal set, $\Psi_k(x_o,y_o) = A_k$, and equation (A.22) can now be written in the form,

$$p(x,y,t/x_o,y_o) = \sum_{j=1}^{\infty} e^{-k_j^2 t}\,\Psi_j(x_o,y_o)\Psi_j(x,y) \tag{A.26}$$

Substitution of this expression into equation (A.3) yields

$$Q(x_o,y_o,t) = \int_R\int \sum_{j=1}^{\infty} e^{-k_j^2 t}\,\Psi_j(x_o,y_o)\Psi_j(x,y)\,dx\,dy \tag{A.27}$$

$$Q(x_o,y_o,t) = \sum_{j=1}^{\infty} e^{-k_j^2 t}\,\Psi_j(x_o,y_o)\int_R\int \Psi_j(x,y)\,dx\,dy \tag{A.28}$$

If $\int_R\int \Psi_j(x,y)\,dx\,dy = B_j$ then

$$Q(x_o,y_o,t) = \sum_{j=1}^{\infty} e^{-k_j^2 t}\,\Psi_j(x_o,y_o)B_j \tag{A.29}$$

Expanding the series,

$$Q(x_o,y_o,t) = e^{-k_1^2 t}\,\Psi_1(x_o,y_o)B_1 + e^{-k_2^2 t}\,\Psi_2(x_o,y_o)B_2 + \ldots\ldots \qquad (A.30)$$

Since the k's are an increasing set of real numbers, for large values of time, the first term of the series is the only significant term and equation (A.30) may be written as follows

$$Q(x_o,y_o,t) \approx e^{-k_1^2 t}\,\Psi_1(x_o,y_o)B_1$$

Taking logarithms of both sides of the equation yields,

$$k_1^2 = \frac{-\ln Q(x_o,y_o,t)}{t} + \frac{\ln \Psi_1(x_o,y_o)B_1}{t} \qquad (A.32)$$

Taking the limit as $t \rightarrow \infty$

$$k_1^2 = \lim_{t \rightarrow \infty} \frac{-\ln Q(x_o,y_o,t)}{t} \qquad (A.33)$$

When finite time t, is involved, the calculation of the lowest eigenvalue of equation (A.1) by means of equation (A.33) is subject to two sources of error. The first is due to neglecting all the terms in the series representation (A.29) after the initial one and the second source of error results from neglecting the quantity $\frac{\ln \Psi_1(x_o,y_o)B_1}{t}$ for the finite values of time since in any computational scheme a finite value of time must be employed. This latter source of error is removed by the following procedure:

Consider equation (A.30) for two large values of time t_1 and t_2, i.e.;

$$Q(x_o, y_o, t) = e^{-k_1^2 t_1} \Psi_1(x_o, y_o) B_1 \tag{A.34}$$

$$Q(x_o, y_o, t) = e^{-k_1^2 t_2} \Psi_1(x_o, y_o) B_1 \tag{A.35}$$

Dividing equation A.35 by equation A.34, one obtains

$$\frac{Q(x_o, y_o, t_2)}{Q(x_o, y_o, t_1)} = e^{-k_1^2 (t_2 - t_1)} \tag{A.36}$$

Taking logarithms again yields

$$k_1^2 = \frac{\ln Q(x_o, y_o, t_1) - \ln Q(x_o, y_o, t_2)}{t_2 - t_1} \tag{A.37}$$

The quantity $Q(x_o, y_o, t)$, representing the probability that a particle which begins a random walk at a point (x_o, y_o) will remain within an absorbing boundary C during the time interval t_1, can be approximated by the following sampling procedure.

Start a particle on a random walk from the point (x_o, y_o) at time $t = 0$. The rules governing the random walk are given by the generalized Langevin Equations A.6, A.7 and A.8. The walk continues for a time t and at the end of this time interval the observation is made as to whether or not the particle has remained within the absorbing boundary C. Perform N_o such random walks and count the numbers of particles N_t which have not left the region during the time interval $(0,t)$. $Q(x_o,y_o,t)$ can be approximated by

$$Q(x_o,y_o,t) \approx \frac{N_t}{N_o} \tag{A.38}$$

The lowest eigenvalue k_1 may now be calculated by the expression

$$k_1^2 = \frac{\ln\frac{N_{t_1}}{N_o} - \ln\frac{N_{t_2}}{N_o}}{t_2 - t_1} \tag{A.39}$$

$$k_1^2 = \frac{\ln \frac{N_{t_1}}{N_{t_2}}}{t_2 - t_1} \tag{A.40}$$

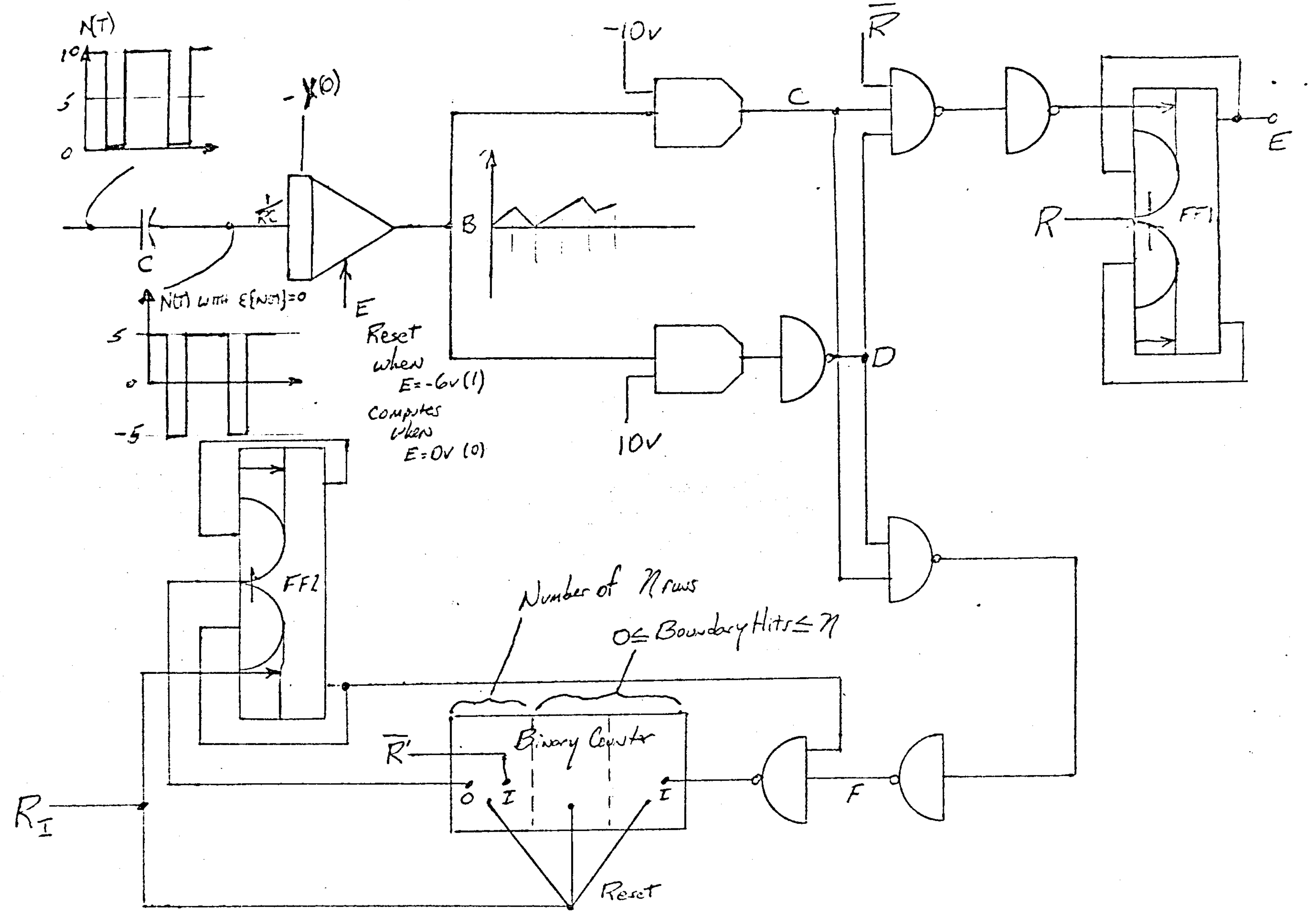

Figure 1 Implementation of One Dimensional Vibrating String Problem

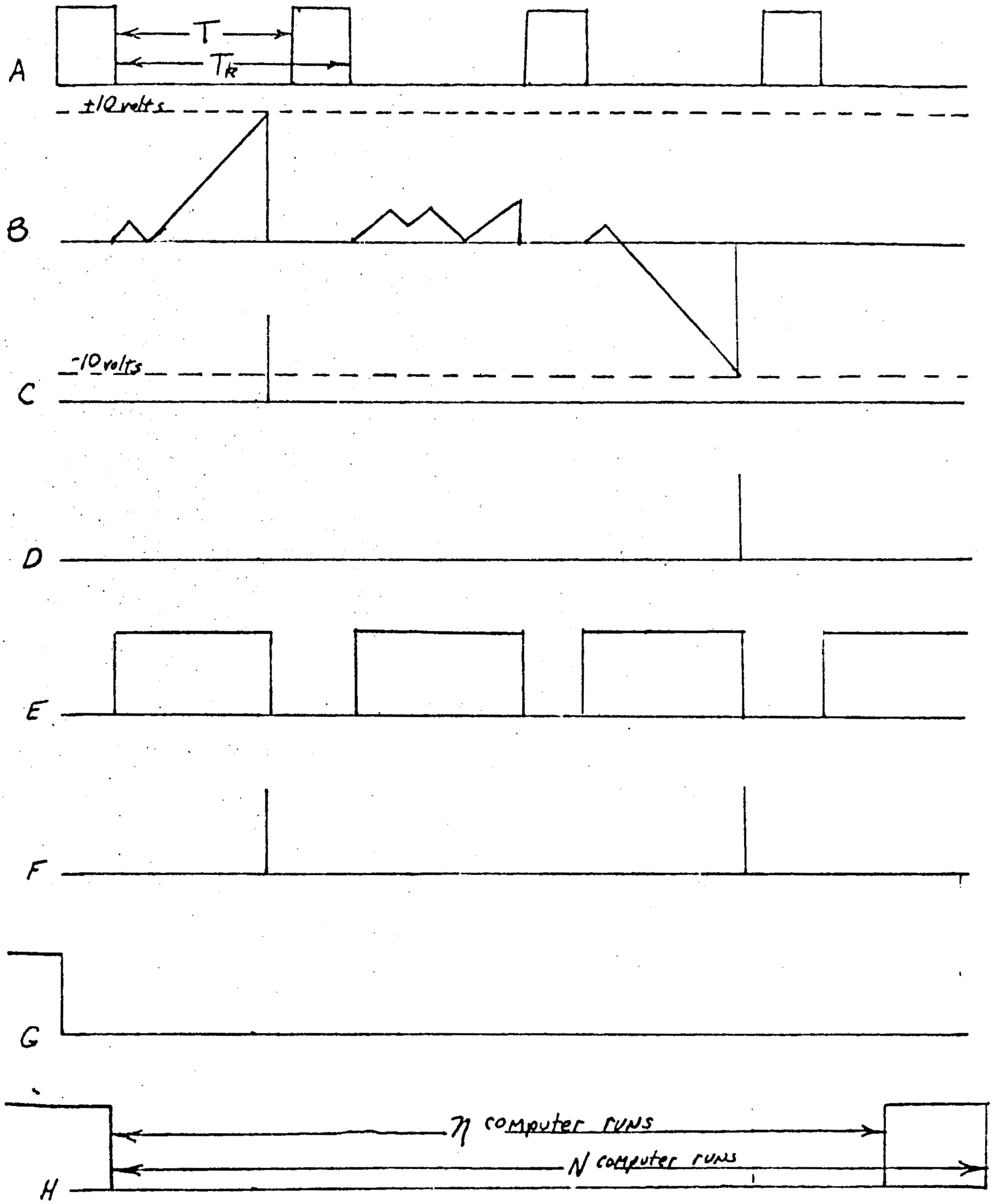

Figure 2 Typical Waveforms

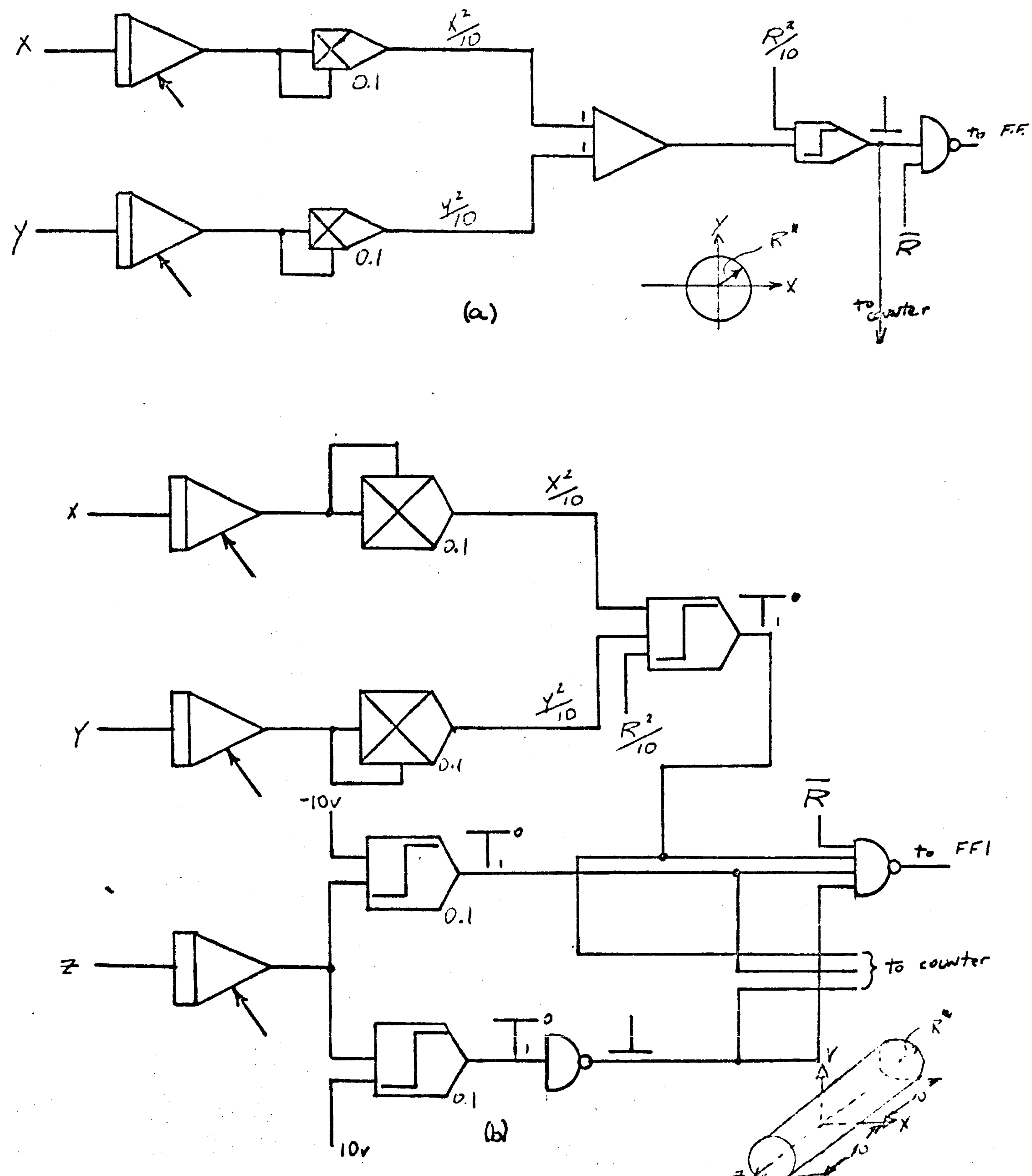

Figure 3 Extension of Example Problem to Two and Three Dimensional Problems. (a) Two Dimensional Circular Membrane; (b) Three Dimensional Cylindrical Body.

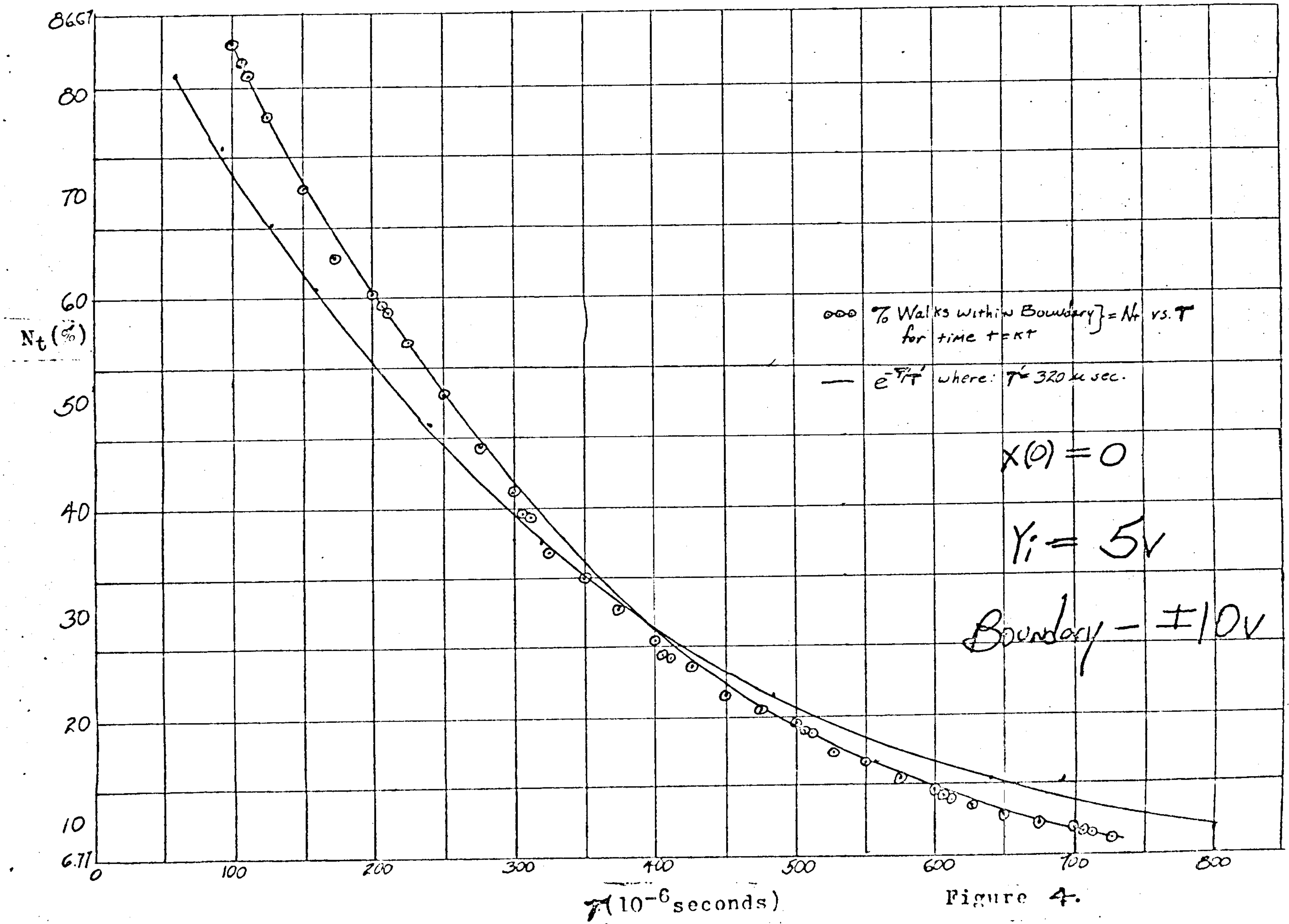

86.67
80
70
60
N_t (%)
50
40
30
20
10
6.71
0
100
200
300
400
500
600
700
800
τ (10^{-6} seconds)
% Walks within Boundary} = N_t vs. τ for time $t = K\tau$
$e^{-\tau/\tau'}$ where: $\tau' = 320\ \mu$ sec.
$X(0) = 0$
$Y_i = 5V$
Boundary - ±10V

Figure 4.

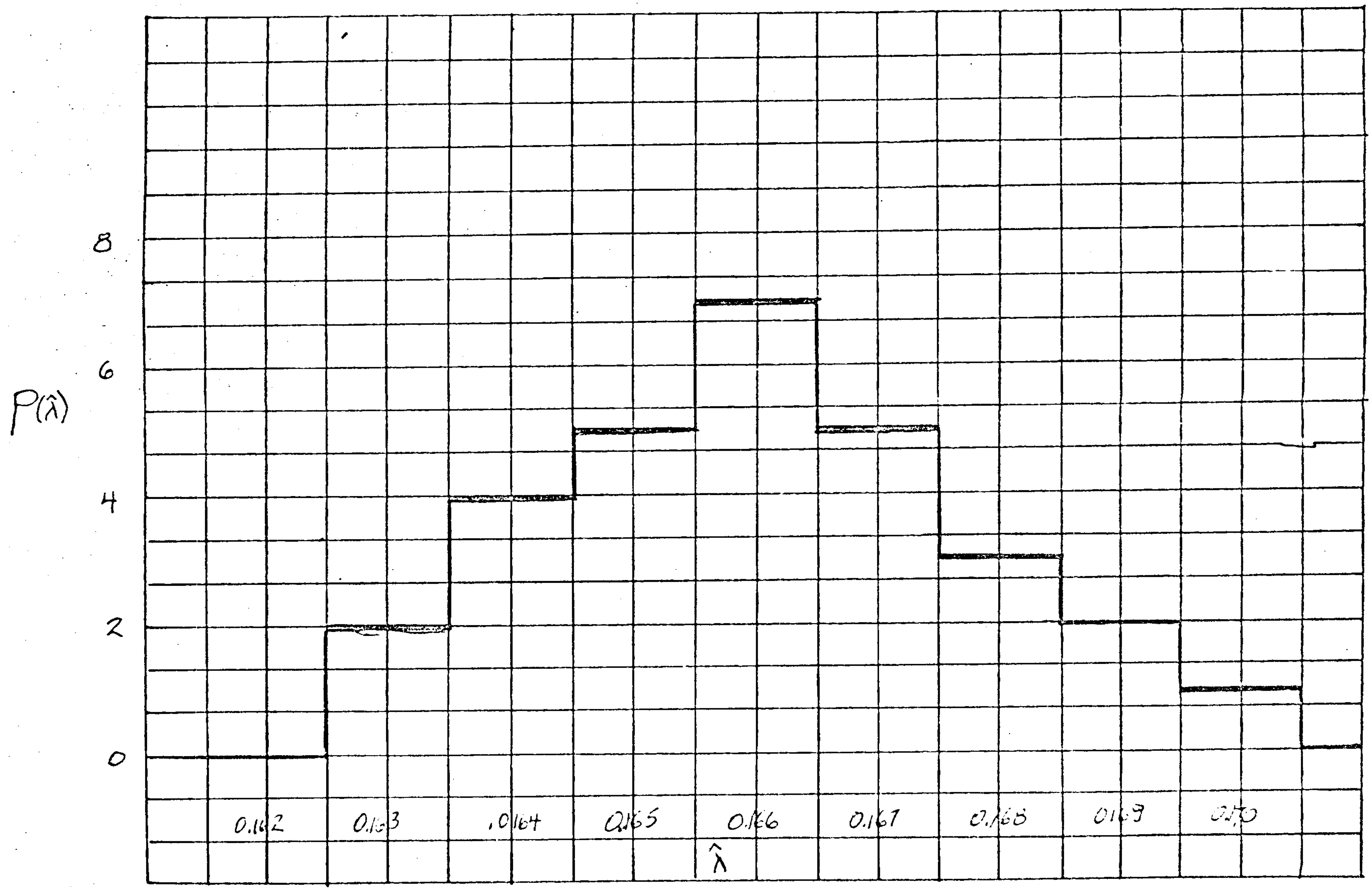

Figure 5. Sample probability density for Vibrating String Example Problem

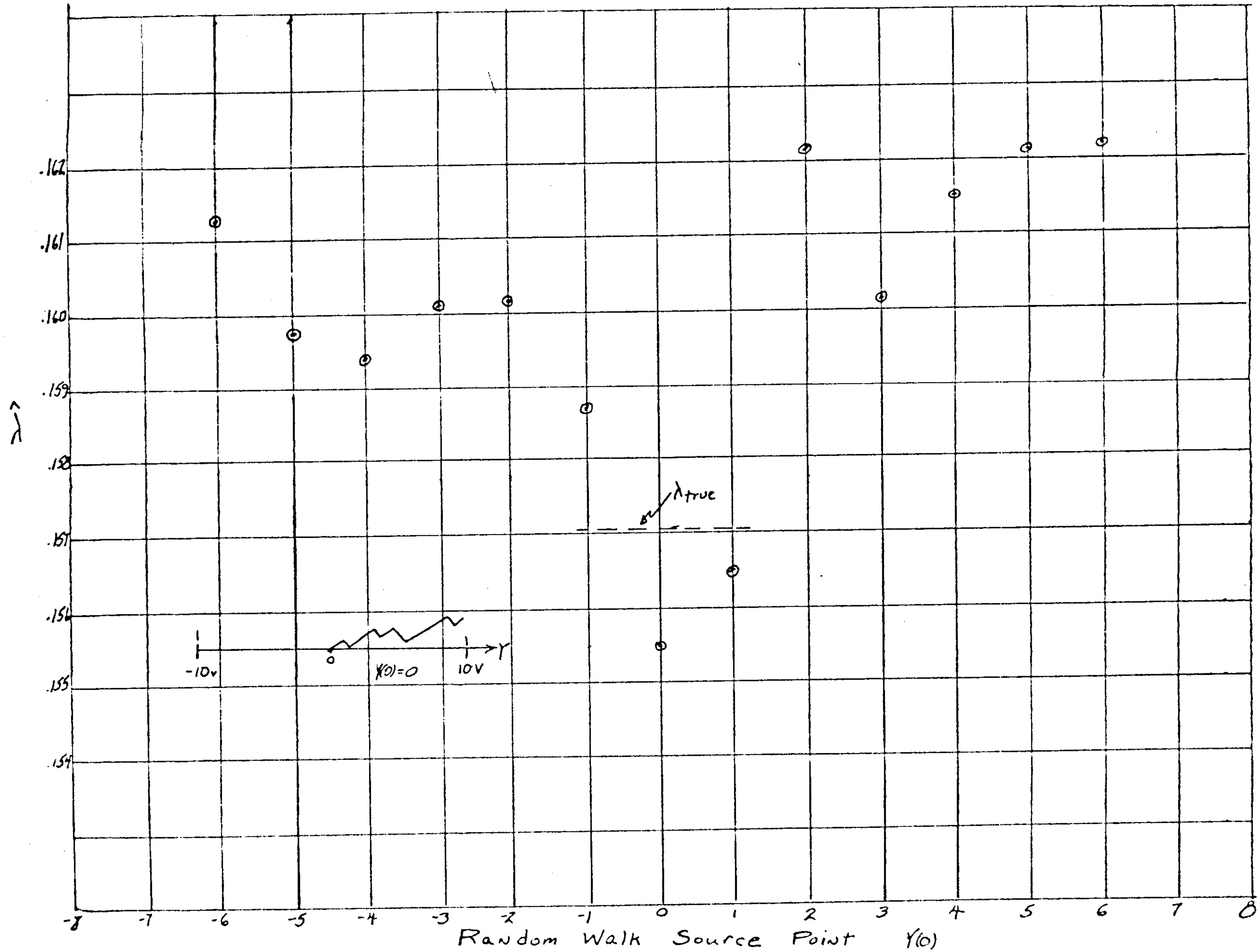

Figure 6

(Should I connect pts?)

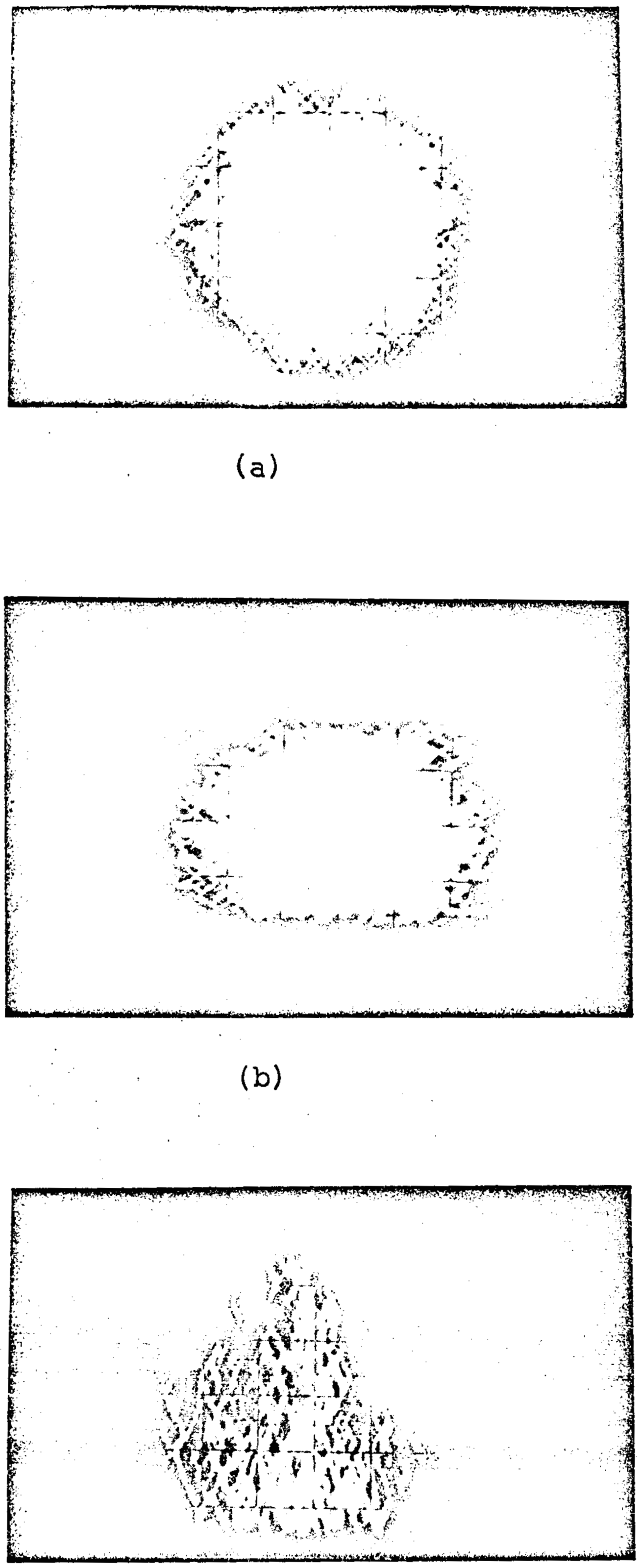

(a)

(b)

(c)

Figure 7. Photographs of Random Walks within (a) Circular, (b) Rectangular and (c) Triangular Boundaries

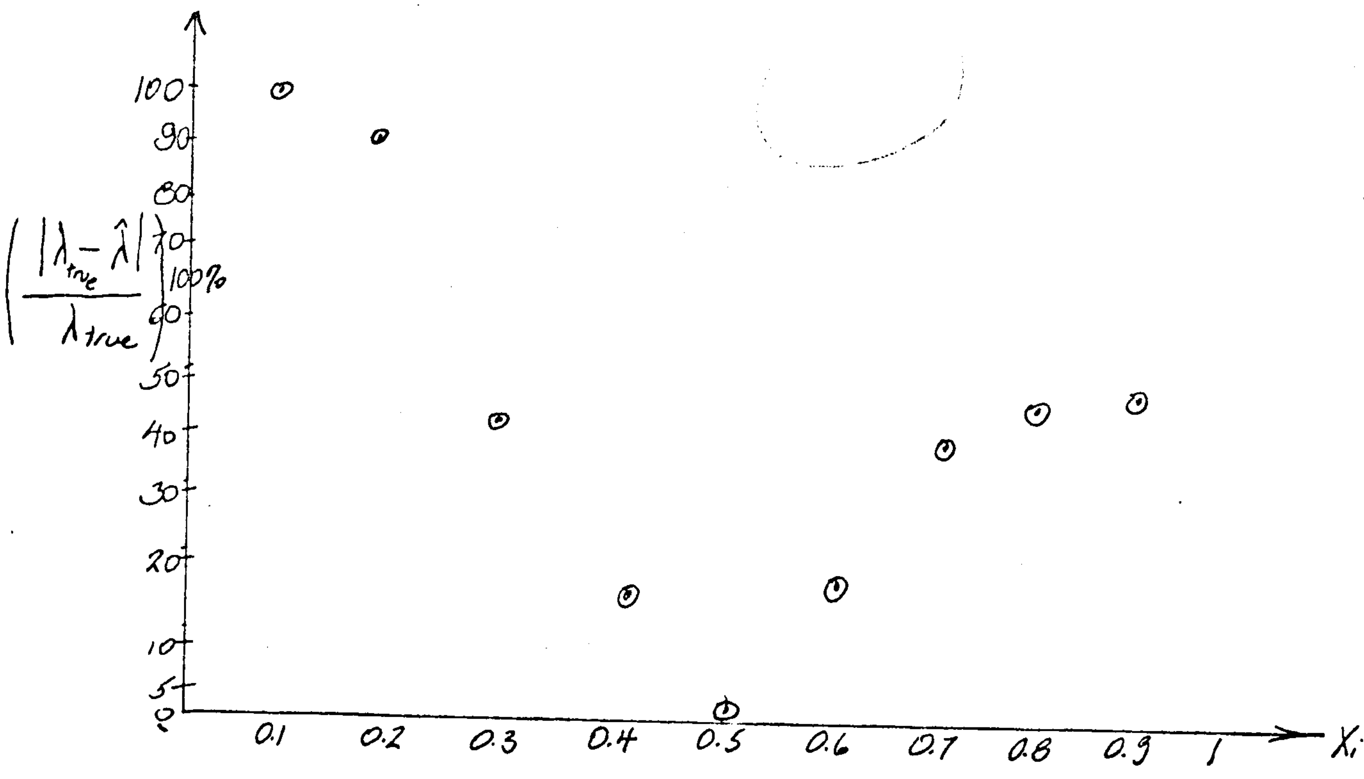

Figure 8

(Should I connect pts?)

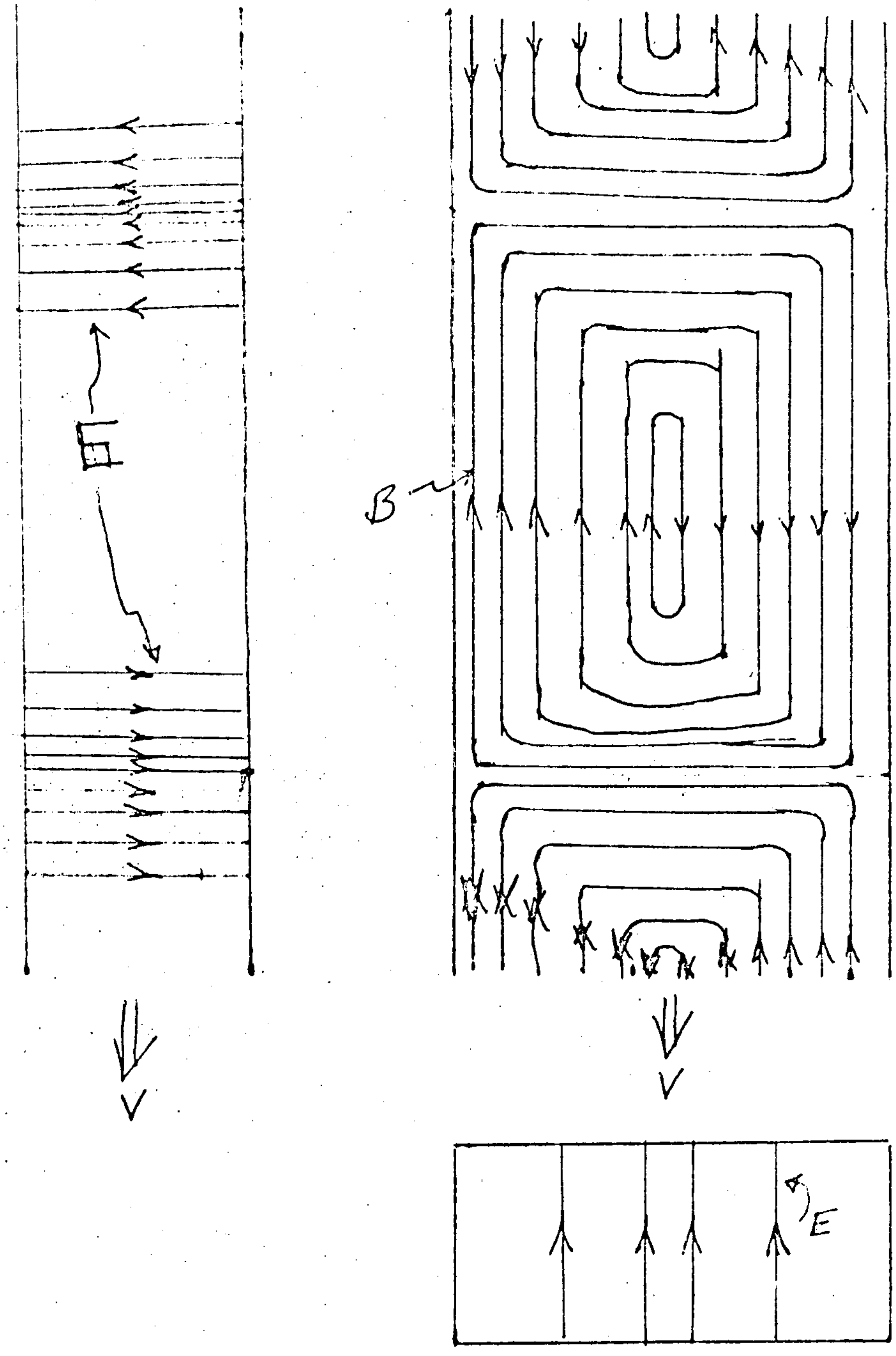

Figure 9 Electromagnetic wave propagating along axial Direction of Rectangular Wave guide

A. One Dimensional Boundary

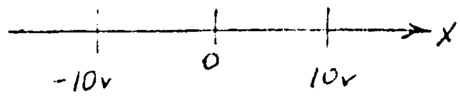

$\lambda_{true} = 0.157079$

B. Two Dimensional Circular Boundary

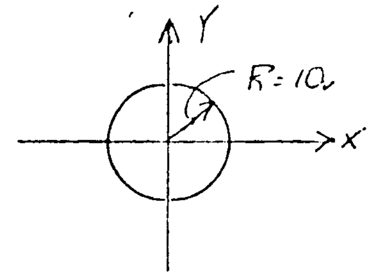

$\lambda_{true} = 0.24048$

C. Two Dimensional Square Boundary

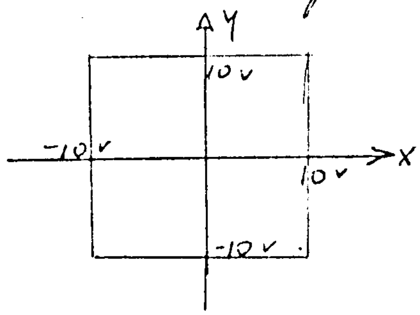

$\lambda_{true} = 0.2214$

D. Two Dimensional Rectangular Boundary

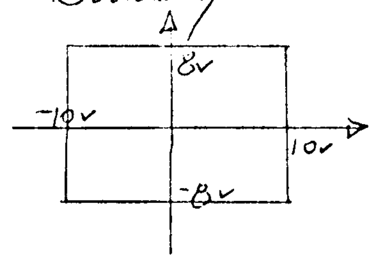

$\lambda_{true} = 0.25132$

E. Two Dimensional Circular Boundary with one Vane

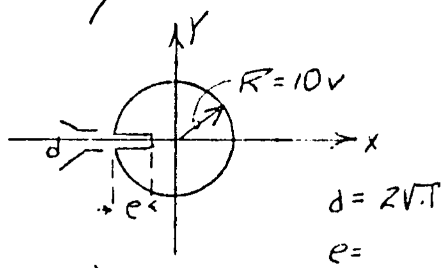

$\lambda_{true}^{(16)} = 0.2163$

F. Three Dimensional Spherical Boundary

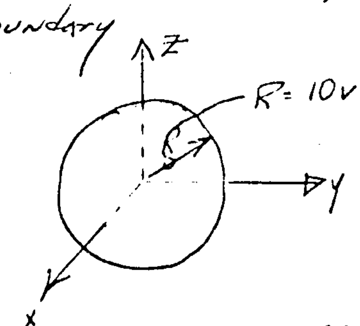

$\lambda_{true} = 0.314159$

G. Three Dimensional Cubical Boundary

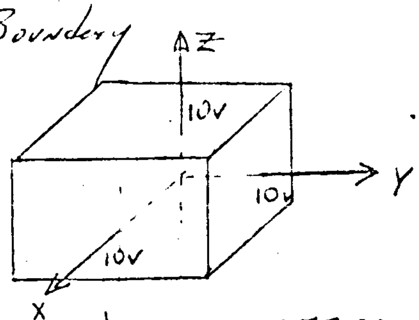

$\lambda_{true} = 0.27208$

H. The Dimensional Cylindrical Boundary

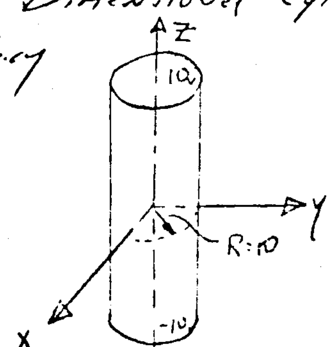

$\lambda_{true} = 0.28723$

Table 1